

# An Independent Robust Modal PID Control Approach for Seismic Control of Buildings

Sadegh Etedali<sup>1\*</sup>, Mohammad Reza Sohrabi<sup>1</sup> and Saeed Tavakoli<sup>2</sup>

<sup>1</sup>Department of Civil Engineering, Faculty of Engineering, University of Sistan and Baluchestan, Zahedan, Iran

<sup>2</sup>Faculty of Electrical and Computer Engineering, University of Sistan and Baluchestan, Zahedan, Iran

\*Corresponding author's Email address: s\_etedali@pgs.usb.ac.ir

**ABSTRACT:** In this paper, an independent robust modal PID control approach for seismic control of structures is proposed. First, state space equations of the structure are transformed into modal coordinates. Second, the parameters of the modal PID control are separately designed in a reduced modal space. To create a good trade-off between the performance and robustness of the modal controller, the modal feedback gain is determined using genetic algorithms. Then, the feedback gain matrix of the controller is obtained based on the contribution of modal responses to the structural response. Considering four earthquakes and twelve performance indices, the performance of the controller is investigated for an 11-story realistic building equipped with ATMD. Simulation results show that the proposed controller significantly performs better than the LQR in reduction of structural responses. Unlike the LQR, the proposed controller is able to significantly reduce structural responses in strong earthquakes at the cost of demanding a higher control force and external power. Furthermore, it maintains appropriate performance in dealing with model uncertainties. In addition, the proposed controller has several advantages over conventional modern controllers in terms of simplicity and reduction of required sensors to the number of controlled stories.

**Keywords:** Seismic Control, Active Tuned Mass Damper, Modelling Error, Robust Control, PID Controller

ORIGINAL ARTICLE

## INTRODUCTION

Structural control methods are modern strategies used to enhance the safety of structures and to improve the habitability of structures subjected to environmental dynamic load such as strong wind and earthquake loads. They can be classified as passive active, semi-active and hybrid control. A structure equipped with active, semi active or hybrid control system is called a smart structure. A smart structure consists of three physical components: sensors, actuators and a computer. The sensor measures the responses of controlled structures along the degrees of freedom and actuator applies the required control force. A control algorithm is also need to determine the magnitude of control force at any given time. The performance of a control device highly depends on the control algorithm applied to adjust control force. There are many strategies and physical systems in structural control. The common goal in them all is to minimize the effects vibrations on structures in real time (Fisco and Adeli, 2011a).

Tuned mass dampers (TMDs) are the oldest passive control devices which have been developed to suppress structural vibrations from environmental disturbances (Yang and Soong, 1988). A TMD have fixed frequency and damping characteristics and can be used to tune only the fundamental frequency of a structure (Datta, 1996). Despite the emergence of nearly four decade-old system in practice, as a modern technology in vibration control of structures, TMD systems have several shortcomings. First, because of

uncertainty in specification of structural model, it is not possible to estimate the fundamental frequency of vibration of a structure accurately. Second, this frequency changes during an extreme dynamic event, such as strong ground motion. Also, TMDs are effective in order to improve structural responses in narrow range of load frequencies (Fisco and Adeli, 2011a).

One of the earliest approaches to active control of structures has been active tuned mass damper (ATMD). In a structure equipped with ATMD system, an actuator placed between the structure and TMD system applies a control force in real time to the structure. ATMD system can significantly reduce the responses of structure; however, the demanded external control force may be extremely large for large or massive buildings. Several researches suggested semi-active tuned mass dampers (SATMDs) to cope with this issue. In this approach, a variable damping device, such as a magneto-rheological (MR) damper, is added to a TMD system to adjust its tuning capability in real time (Fisco and Adeli, 2011a). However, control algorithms developed for active control can directly be used for developing other control strategies such as semi-active and hybrid control. Therefore, despite some obvious problems in implementation of an active control strategy for buildings, the research in the area of active structural control is still continuing. Different control algorithms have been proposed to improve the performance of smart buildings. The most common control algorithms are

LQR, LQG, independent modal space control, sliding mode control,  $H_2$ , and  $H_\infty$  (Datta, 1996; Yang and Soong, 1988; Sarbjeet and Datta, 2000; Ha, 2001; Fisco and Adeli, 2011b; Samali and Al-Dawod, 2003; Samali et al., 2004; Pourzeynali et al., 2007; Huo, 2008; Park and Park, 2012).

Modeling errors may adversely affect the stability and performance of a control system (Gu et al., 2005). Un-modeled dynamics, neglected nonlinearities, model order reduction and variation of system parameters are the important sources of modeling errors in structures. Some of conventional control algorithms such as linear quadratic regulator (LQR) and linear quadratic gaussian (LQG), ignore modeling errors. Usually, these methods have good performance for nominal models; however, control objectives are not satisfied for actual systems. Therefore, these methods may be faced with numerous problems in practice and they cannot obtain pre-specified control objectives. In recent years, considering the effect of modelling errors on vibration control of structures equipped with ATMD, many control algorithms have been proposed by several researches (Samali and Al-Dawod, 2003; Samali et al., 2004; Pourzeynali et al., 2007; Huo, 2008).

By review of control algorithms used in industries, PID controllers are known as the most popular industrial controllers, Because of its remarkable effectiveness and simplicity of implementation. Although significant developments have been made in advanced control theory, according to the literature, more than 95% of industrial controllers are still PID (Tavakoli et al., 2006). Although this controller widely used in industrial control systems, there are few studies on using PID controller for vibration control of structures. In order to control the vibration of the plates and beams using smart materials and control devices, the application of PID controllers have been studied by several researchers (Shen et al., 2000; Jung et al., 2004; Fung et al., 2005). Guclu (2003) used both an FLC and a PD controller to seismic control of an active control device in a 5-story structure. Moreover, he developed both a sliding-mode controller and a PID controller for a building equipped with ATMD system and evaluated performance of the proposed controller to Marmara earthquake (Guclu, 2006). Guclu and Yazici (2007) applied a PID controller for a nonlinear structural system and assessed its performance to Kococeli earthquake. Also, they designed a fuzzy PID controller to control a 15-story building equipped with ATMD system (Guclu and Yazici, 2009). According to the previous researches on the performance of PID controller on structural vibrations, the researches considered their proposed PID controller for only one earthquake, whereas during the lifetime of structures, different load disturbances may be imposed on structures. As different earthquakes have different frequency spectrums, there was no guarantee that a controller tuned to reject an earthquake could perform well in rejecting other earthquakes. Also, in these studies, the researchers have not paid attention to modeling errors and its effect on the performance of the proposed controller. Aguirre et al. (2011) suggested a PI controller to minimize the structural responses a 3-story building equipped with MR dampers. Etedali et al. (2013) developed optimal PD/PID controllers for seismic

control of a benchmark isolated structure equipped with piezoelectric friction dampers. They demonstrated that PD/PID controllers performed better in terms of simultaneous reduction of the floor acceleration and maximum displacement of the isolator in comparison with the maximum passive operation and LQG methods.

A key element in successful implementation of smart structure technology is an effective control algorithm to adjust the control forces to be applied to the structure. Because civil structures are large and complex and external dynamic loadings are unknown and varied, there are uncertainties in structural model and load disturbance. An effective control algorithm has to be robust and function under various dynamic conditions. As a result, an effective control algorithm has to be robust and function under various dynamic conditions. In this paper, an independent robust modal control approach based on the PID controller is presented. This strategy can prevent excessive trial and error designs in conventional modern control methods and simplify control process. Also, the proposed controller is able reduces the number of the required sensors of the control system to the number of controlled stories. Therefore, the proposed controller provided a simple control system with advantages in terms of reliability and cost compared with the conventional control modern methods such as LQR and LQG. The proposed controller is applied toward the active control of an 11-story realistic building equipped with ATMD. In numerical studies, four well known earthquakes and 12 performance indices are used to evaluate performance of the proposed controller. In order to survey sensitivity the proposed control to model uncertainties, the robustness of the controller has been demonstrated through the uncertainty in the parameters of the structure. Furthermore, to assessment the performance of the proposed controllers, their results are compared with LQR controller.

## AN OVERVIEW OF PID CONTROL

PID controller is a generic control loop feedback controller widely used in industrial control systems. Figure 1 shows a block diagram of closed-loop control for a single degree of freedom system.

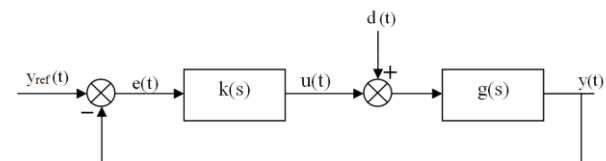


**Figure 1.** Block diagram of closed-loop control for a single degree of freedom system

$G(s)$  is transfer function of the structural system and  $k(s)$  is the PID controller in  $S$  domain.  $y(t)$  is output of the plant which denotes response of the structure. Output of the controller is  $u(t)$ ,  $d(t)$  is load disturbance applied to the system, simulating an earthquake dynamic force,  $y_{ref}(t)$  is the reference value, which represents the desired feedback of the controller. Also,  $e(t)$  is the error vector, which is the difference between reference value and value of the output. In structural control, it can be assumed that  $y_{ref}(t)=0$ , therefore,  $e(t)=y(t)$ .

The transfer function of a PID controller is given by Eq. (1). The control force vector,  $u_{PID}(t)$ , is determined using Eq. (2). Parameter  $t$  is duration of the occurrence of an earthquake.

$$K(s)_{PID} = k_c \left( 1 + \frac{1}{\tau_i s} + \tau_d s \right) \quad (1)$$

$$u_{PID}(t) = k_c \left[ e(t) + \frac{1}{\tau_i} \int_0^t e(t) dt + \tau_d \frac{de(t)}{dt} \right] \quad (2)$$

The Parameters of PID controller are proportional gain,  $k_c$ , integral term,  $\tau_i$ , and differential term,  $\tau_d$ . Proportional gain takes an immediate corrective measure as soon as an error is detected; however, using only proportional controller a steady state error happens after a change in the load disturbance. Integral term can eliminate the steady state error. A disadvantage of integral action is that it tends to have a destabilizing effect. A limited amount of oscillation can be usually tolerated because of being often associated with a faster response. The derivative term tends to stabilize the closed-loop system and increase damping of the system. However, derivative action often leads to large control actions (Tavakoli, 2005).

### Seismic control of structures using pid controller

Equation of motion of an n-degree-of-freedom linear structure subjected to earthquake ground acceleration  $\ddot{x}_g(t)$  is given by

$$\mathbf{M}\ddot{\mathbf{x}}(t) + \mathbf{C}\dot{\mathbf{x}}(t) + \mathbf{K}\mathbf{x}(t) = -\mathbf{M}\mathbf{r}\ddot{x}_g(t) \quad (3)$$

where  $\mathbf{M}$ ,  $\mathbf{C}$  and  $\mathbf{K}$  refer to  $n \times n$  mass, damping and stiffness matrices, respectively.  $\mathbf{x}(t)$ ,  $\dot{\mathbf{x}}(t)$  and  $\ddot{\mathbf{x}}(t)$  are  $n \times 1$  displacement, velocity and acceleration vectors, respectively. Also,  $\mathbf{r} = [1, 1, \dots, 1]^T$  is  $n \times 1$  seismic influence vector. When control force,  $\mathbf{u}(t)$ , are applied to the structure, the equation of motion can be written as

$$\mathbf{M}\ddot{\mathbf{x}}(t) + \mathbf{C}\dot{\mathbf{x}}(t) + \mathbf{K}\mathbf{x}(t) = -\mathbf{M}\mathbf{r}\ddot{x}_g(t) + \mathbf{D}\mathbf{u}(t) \quad (4)$$

where  $\mathbf{D}$  represents an  $n \times n_c$  location matrix of control forces and  $\mathbf{u}(t)$  is an  $n_c \times 1$  control force vector of  $n_c$  actuators. In the closed loop control of a structure, when velocity of a story is feedback, the proportional gain, integral term and differential terms of the PID controller modify damping, stiffness and mass of the structure, respectively.

Considering Eq. (2), to determine control force of any controlled story, a sensor and two computational resources are required for measuring and computing displacement, velocity and acceleration of the story. The controlled story is the story which is equipped with actuator to apply control force to it. Therefore, the PID control force of actuator installed in the j-th story,  $u_{PIDj}(t)$ , is given by Eq.(5).

$$u_{PIDj}(t) = \mathbf{G}_j \mathbf{W}_j(t) \quad (5)$$

where  $\mathbf{G}_j$  is  $1 \times 3$  feedback gain vector and  $\mathbf{W}_j$  is  $3 \times 1$  feedback vector of controller in the j-th story.

Considering Eq. (2), when velocity of a story is feedback,  $\mathbf{G}_j$  and  $\mathbf{W}_j$  are obtained as

$$\mathbf{G}_j = k_{c_j} \begin{bmatrix} 1 & \tau_{d_j} \\ \tau_{i_j} & \end{bmatrix} = \begin{bmatrix} G_{I_j} & G_{P_j} & G_{D_j} \end{bmatrix} \quad (6)$$

$$\mathbf{W}_j(t) = [x_j(t) \quad \dot{x}_j(t) \quad \ddot{x}_j(t)]^T$$

where  $k_{c_j}$ ,  $\tau_{i_j}$  and  $\tau_{d_j}$  present the proportional gain, integral term and the differential term of the PID controller of the j-th story, respectively. Also,  $x_j(t)$ ,  $\dot{x}_j(t)$  and  $\ddot{x}_j(t)$  refer to displacement, velocity and acceleration of the j-th story, respectively. Considering Eq. (5), the control force vector of structure,  $\mathbf{u}(t)$ , is given by

$$\mathbf{u}(t) = \mathbf{G}_c \mathbf{W}_c(t) \quad (7)$$

Where  $\mathbf{G}_c$  is the  $n_c \times 3n_c$  feedback gain matrix and  $\mathbf{W}_c(t)$  is the  $3n_c \times 1$  feedback vector of the controller of structure. Considering Eq. (6),  $\mathbf{G}_c$  and  $\mathbf{W}_c(t)$  are expressed as

$$\mathbf{G}_c = \begin{bmatrix} \mathbf{G}_{I_c} & \mathbf{G}_{P_c} & \mathbf{G}_{D_c} \end{bmatrix} \quad (8)$$

$$\mathbf{w}_c(t) = [\mathbf{x}_c(t) \quad \dot{\mathbf{x}}_c(t) \quad \ddot{\mathbf{x}}_c(t)]^T$$

where  $\mathbf{G}_{I_c}$ ,  $\mathbf{G}_{P_c}$  and  $\mathbf{G}_{D_c}$  are  $n_c \times n_c$  matrices given by

$$\mathbf{G}_{I_c} = \text{diag}(G_{I_1}, G_{I_2}, \dots, G_{I_{n_c}})$$

$$\mathbf{G}_{P_c} = \text{diag}(G_{P_1}, G_{P_2}, \dots, G_{P_{n_c}}) \quad (9)$$

$$\mathbf{G}_{D_c} = \text{diag}(G_{D_1}, G_{D_2}, \dots, G_{D_{n_c}})$$

Also,  $\mathbf{x}_c(t)$ ,  $\dot{\mathbf{x}}_c(t)$  and  $\ddot{\mathbf{x}}_c(t)$  refer to  $n_c \times 1$  displacement, velocity and acceleration vectors of the controlled stories, respectively.

### Independent robust modal pid control approach

A robust modal-PID control approach is developed for seismic control of structures in this section. This controller is a hybrid control algorithm combining PID controller with a control method based on modal space. This approach consists of two phases. In the first phase, n coupled equations of motion of an n-degree-of-freedom structure are transformed into a set of n decoupled equations. They can be expressed as second-order models of structural modes in the modal coordinates. In the second phase, at first, parameters of the robust PID controller are separately determined for selected modes of structure using an optimization procedure based on genetic algorithms. Then, according to the contribution of the modal responses to the structural response, the gain feedback matrix,  $\mathbf{G}_c$ , of control system is calculated.

#### Phase 1

The equation of motion of the structure expressed in Eq. (4) is a set of  $n$  simultaneous differential equations, which are coupled by the off-diagonal terms in the mass and stiffness matrices. These equations can transform into a set of  $n$  independent normal coordinate equations in modal space. For this purpose, it is assumed that the coordinate transformation in the modal space is based on Eq. (10).

$$\mathbf{x}(t) = \Phi \mathbf{y}(t) \quad (10)$$

where  $\mathbf{y}(t) = [y_1(t), y_2(t), \dots, y_n(t)]^T$  is modal displacement vector and  $\Phi$  is  $n \times n$  orthonormalized mode shape matrix relative to the mass matrix. The results of this type of normalizing is the following relations

$$\begin{aligned} \Phi^T \mathbf{M} \Phi &= \mathbf{I} \\ \Phi^T \mathbf{K} \Phi &= \Omega^2, \quad \Omega = \text{diag}(\omega_1, \omega_2, \dots, \omega_n) \\ \Phi^T \mathbf{C} \Phi &= \mathbf{C}_m = \text{diag}(2\xi_1\omega_1, 2\xi_2\omega_2, \dots, 2\xi_n\omega_n) \end{aligned} \quad (11)$$

where  $\omega_i$  and  $\xi_i$  are the natural frequency and modal damping ratio of the  $i$ -th mode. By using Eqs. (10) and (11), Eq. (4) can be described in the modal space as follows

$$\ddot{\mathbf{y}}(t) + \mathbf{C}_m \dot{\mathbf{y}}(t) + \Omega^2 \mathbf{y}(t) + \Phi^T \mathbf{M} \mathbf{r} \ddot{x}_g(t) = \mathbf{u}_m(t) \quad (12)$$

where  $\mathbf{u}_m(t)$  is the  $n \times 1$  modal control force vector given by

$$\mathbf{u}_m(t) = \Phi^T \mathbf{D} \mathbf{u}(t) \quad (13)$$

On the other hand, the modal control force vector,  $\mathbf{u}_m(t)$ , can be present as

$$\mathbf{u}_m(t) = \mathbf{G}_m \mathbf{W}_m(t) \quad (14)$$

where  $\mathbf{G}_m$  is the  $n \times 3n$  modal feedback gain matrix and  $\mathbf{W}_m(t)$  is the  $3n \times 1$  modal feedback vector of the controller in the modal space. Considering the parameters of PID controller in each mode,  $\mathbf{G}_m$  and  $\mathbf{W}_m(t)$  are given by

$$\begin{aligned} \mathbf{G}_m &= \begin{bmatrix} \mathbf{G}_{I_m} & \mathbf{G}_{P_m} & \mathbf{G}_{D_m} \end{bmatrix} \\ \mathbf{w}_m(t) &= [\mathbf{y}_m(t) \quad \dot{\mathbf{y}}_m(t) \quad \ddot{\mathbf{y}}_m(t)]^T \end{aligned} \quad (15)$$

where  $\mathbf{G}_{I_m}$ ,  $\mathbf{G}_{P_m}$  and  $\mathbf{G}_{D_m}$  are the  $n \times n$  matrices, which are given by

$$\begin{aligned} \mathbf{G}_{I_m} &= \text{diag}(G_{I_1}, G_{I_2}, \dots, G_{I_n}) \\ \mathbf{G}_{P_m} &= \text{diag}(G_{P_1}, G_{P_2}, \dots, G_{P_n}) \\ \mathbf{G}_{D_m} &= \text{diag}(G_{D_1}, G_{D_2}, \dots, G_{D_n}) \end{aligned} \quad (16)$$

Also,  $\mathbf{y}_m(t)$ ,  $\dot{\mathbf{y}}_m(t)$  and  $\ddot{\mathbf{y}}_m(t)$  refer to the  $n \times 1$  modal displacement, modal velocity and modal acceleration

vectors, respectively. Considering the term  $\Phi^T \mathbf{M} \mathbf{r} \ddot{x}_g(t)$  in Eq. (12) as the load disturbance which must be applied to the structure, Eq. (12) can be written in the state space as follows

$$\dot{\mathbf{q}}(t) = \begin{bmatrix} \mathbf{0} & \mathbf{I} \\ -\Omega^2 & -\mathbf{C}_m \end{bmatrix} \mathbf{q}(t) + \begin{bmatrix} \mathbf{0} \\ \mathbf{I} \end{bmatrix} \mathbf{u}_m(t) \quad (17)$$

where  $\mathbf{q}(t) = [\mathbf{y}(t) \quad \dot{\mathbf{y}}(t)]^T$  is the modal state vector. Considering Eq. (17), the state space equation of the  $i$ -th mode of structure is given by

$$\dot{\mathbf{q}}_{mi}(t) = \begin{bmatrix} 0 & 1 \\ -\omega_i^2 & -2\xi_i\omega_i \end{bmatrix} \mathbf{q}_{mi}(t) + \begin{bmatrix} 0 \\ 1 \end{bmatrix} u_{mi}(t) \quad (18)$$

where  $\mathbf{q}_{mi} = [y_i(t) \quad \dot{y}_i(t)]^T$  is the modal state vector of the  $i$ -th mode. Also, the state space equation of the  $i$ -th mode expressed by Eq. (18) can be described in the frequency domain using a second-order model as shown in Eq. (19).

$$g_{mi}(s) = \frac{1}{s^2 + 2\xi_i\omega_i s + \omega_i^2} \quad (19)$$

## Phase 2

The second phase included two subsections. For second-order models corresponding to selected modes of structure, the parameters of modal PID controller are designed using optimization process. Then, according to the contribution of modal responses to the structural response, the feedback gain matrix is obtained.

### Tuning of modal PID parameters for second order models

The lower order modes of a structure subjected to seismic load usually are the greatest contribution to structural response. Therefore, it is reasonable to truncate analysis when the number of mode is sufficient. In other words, a control system can be designed in the reduced modal space. Equation (17) is a set of  $n$  decoupled modal state equations. By adopting only  $n_{mc}$  ( $n_{mc} < n$ ) modal equations from Eq. (17),  $n_{mc}$  independent state space equations are obtained.

The relationship between the input and output of the controller in the  $i$ -th mode can be identified by Eq. (20).

$$q_{mi}(s) = g_{mi}(s)k_{mi}(s) \quad (20)$$

where  $k_{mi}(s)$  and  $q_{mi}(s)$  are control force and output of the controller in the  $s$ -domain corresponding to the  $i$ -th mode, respectively. Considering Eq. (1), control force of the  $i$ -th mode in the  $s$ -domain,  $K_{mi}(s)$ , is achieved as

$$k_{mi}(s) = k_{c_{mi}} \left( 1 + \frac{I}{\tau_{i_{mi}} s} + \tau_{d_{mi}} s \right) \quad (21)$$

where  $k_{c_{mi}}$ ,  $\tau_{i_{mi}}$  and  $\tau_{d_{mi}}$  are proportional gain, integral term and differential term of the PID controller in the  $i$ -th mode of structure.

Considering Eq. (21) in the time domain, the control force in the  $i$ -th mode can be obtained as

$$u_{mi}(t) = \mathbf{G}_{mi} \mathbf{W}_{mi}(t) \quad (22)$$

where  $\mathbf{G}_{mi}$  is the  $1 \times 3$  modal feedback gain vector and  $\mathbf{W}_{mi}(t)$  is the  $3 \times 1$  modal feedback vector of the controller in the  $i$ -th mode. These vectors can be given by determining parameters of the PID controller in each of the selected modes as follows

$$\mathbf{G}_{mi} = k_{c_{mi}} \begin{bmatrix} 1 & 1 & \tau_{d_{mi}} \\ \tau_{i_{mi}} & & \end{bmatrix} = [\mathbf{G}_{I_{mi}} \quad \mathbf{G}_{P_{mi}} \quad \mathbf{G}_{D_{mi}}] \quad (23)$$

$$\mathbf{w}_{mi}(t) = [y_{mi}(t) \quad \dot{y}_{mi}(t) \quad \ddot{y}_{mi}(t)]^T$$

where  $y_{mi}(t)$ ,  $\dot{y}_{mi}(t)$  and  $\ddot{y}_{mi}(t)$  refer to modal displacement, velocity and acceleration of structure in the  $i$ -th mode, respectively.

There are many good regulation rules and strategies to determine parameters of the PID controller of a second-order model in the literature (Panda et al., 2004; Skogestad, 2004). These strategies are able to provide both adequate set point regulation and appropriate load disturbance rejection in control processes. Numerical optimization techniques are useful and power tools for tuning of the PID controller for the second-order models. Among of optimization techniques, genetic algorithms (GAs) are able to handle complex problems and, therefore, have significantly broadened the scope of optimization. In contrast to conventional search techniques, GAs are capable of evolving multiple solutions simultaneously (Deb, 2001).

Typically, two objectives should be considered to design an effective controller for seismic control of structures. The first objective is good load disturbance rejection. Earthquakes and strong winds are the load disturbances which may be apply to structures. An effective controller is also important to have good performance and robustness. The performance of controller can relate an acceptable level of structural responses and required control force. Also, a controller is referred to as robust if it is insensitive to model uncertainties. An appropriate trade-off between conflicting the performance and robustness of controller has to be provided.

### Load disturbance rejection

Dynamic loads such as earthquakes or strong winds are random in general and not predictable. Considering seismic events as probabilistic events, it is required several time-history analyses to access reliable results. In stochastic analysis, spectral density function can be used instead of a collection of input time-histories; therefore, the proposed controller employs stochastic analysis method for modeling earthquakes in the frequency domain. Ground artificial acceleration, used for modeling earthquakes, produced by a band limited Gaussian white noise known as filter models. To model the ground acceleration, one well-known filter was introduced by Kanai-Tajimi (1961). By considering several earthquakes, Nagarajaiah and Narasimhan (2006) introduced a modified form of Kanai-Tajimi filter and proposed to apply a white noise according to Eq. (24). The output of this filter simulates the earthquake.

$$F(s) = \frac{4\xi_g \omega_g S}{S^2 + 2\xi_g \omega_g S + \omega_g^2} \quad (24)$$

$$\omega_g = 2\pi \text{ rad/s}, \quad \xi_g = 0.3$$

### Trade-off between performance and robustness of controller

In this paper, parameters of the PID controller in each mode are determined using optimization procedure based on the genetic algorithms. The product of this process is determine of modal feedback gain vector,  $\mathbf{G}_{mi}$ , for the  $i$ -th mode of structure. For this purpose, a suitable objective function must be defined to tune the parameters of controllers in each mode. In the proposed controller, the gain feedback matrix of control system is obtained based on the contribution of the modal responses to the structural responses of controlled structure. Therefore, the optimization problem is related to minimize modal structural responses. Additionally, the objective function must be referred to as finding the acceptable levels of control forces. Moreover, an effective controller must be robust. In other words, it is not sensitive to model uncertainties. Due to model errors, there is difference between frequencies and damping ratios of each mode of nominal structure and the corresponding values of actual structure. Therefore, the values cannot be accurately determined. A commonly-used criterion to consider the sensitivity to modelling errors is the maximum sensitivity. The maximum sensitivity,  $M_s$ , is defined as inverse of the shortest distance from the Nyquist curve of the loop transfer function to the critical point.  $M_s$  is given by

$$M_s = \max_{0 \leq \omega \leq \infty} |S(j\omega)| = \max_{0 \leq \omega \leq \infty} \left| \frac{1}{1 + g(j\omega)k(j\omega)} \right| \quad (25)$$

Typical values of  $M_s$  are in the range of 1.2 to 2. A trade-off should be made between control goals. Smaller values of  $M_s$  result in better robustness while larger ones lead to faster responses. A good balance between these confliction objectives is provided by setting the maximum sensitivity as equal to 1.6 (Tavakoli et al., 2005, Astrom and Hagglund, 1995).

Considering the above-mentioned goals, the objective function applied to determine the parameters of PID controller in each mode can be expressed by Eq. (26)

$$\begin{cases} \text{Min} & I_i = \sum_{k=1}^m w_k I_k \\ \text{S.t} & M_{si} - 1.6 \leq 0 \end{cases} \quad (26)$$

where  $w_k$  ( $k=1, \dots, m$ ) are weighting factors.  $I_k$  ( $k=1, \dots, m$ ) are normalized values of modal structural responses. The most important seismic response of structures is related to stories displacement, drift and acceleration. Therefore,  $I_k$  can be consist of the maximum modal displacement, drift and acceleration, as well as, the root mean square (RMS) of them in controlled second-order models normalized by them corresponding values in the uncontrolled second order

models. Moreover, they can be presented the maximum control force of second-order models normalized by the maximum base shear in the controlled second-order model and its RMS for access to a desirable level of control forces. The uncontrolled second-order model is a second-order model with no control force feedback. An important issue in robust control is to specify the class of alternative models. When the alternative models are specified, the next issue is how to design a control rule to access a robust controller. Many engineering applications have specific performance objectives which must be maintained while a penalty function penalizing deviations is not clearly defined; therefore, to take robustness issues into account, a penalty function is added to the objective function defined in Eq. (26), when the value of maximum sensitivity,  $M_S$  is greater than a predefined value.

### Feedback gain matrix

In this section, the feedback gain matrix,  $\mathbf{G}_c$ , is determined. By formation this matrix, the control forces of actuators in real times can determine according to Eq. (7). If only  $n_{mc}$  modes of the structure is adapted to control of structure, Eqs. (13) and (14) can be rewritten, respectively, for  $n_{mc}$  modes as follows

$$\mathbf{u}_{mc}(t) = \Phi_{mc}^T \mathbf{D} \mathbf{u}(t) \quad (27)$$

$$\mathbf{u}_{mc}(t) = \mathbf{G}_{mc} \mathbf{W}_{mc}(t) \quad (28)$$

where  $\Phi_{mc}$  is the  $n \times n_{mc}$  matrix of the selected  $n_{mc}$  shape modes and  $\mathbf{u}_{mc}$  is the  $n_{mc} \times 1$  modal control force vector of the selected  $n_{mc}$  modes. Also,  $\mathbf{G}_{mc}$  is the  $n_{mc} \times 3n_{mc}$  modal feedback gain matrix and  $\mathbf{W}_{mc}(t)$  is the  $3n_{mc} \times 1$  modal feedback vector of the controller for the selected  $n_{mc}$  modes.

By determining parameters of the PID controller in each mode,  $\mathbf{G}_{mc}$  and  $\mathbf{W}_{mc}(t)$  are given by

$$\mathbf{G}_{mc} = \begin{bmatrix} \mathbf{G}_{I_{mc}} & \mathbf{G}_{P_{mc}} & \mathbf{G}_{D_{mc}} \end{bmatrix} \quad (29)$$

$$\mathbf{w}_{mc}(t) = [\mathbf{y}_{mc}(t) \quad \dot{\mathbf{y}}_{mc}(t) \quad \ddot{\mathbf{y}}_{mc}(t)]^T$$

where  $\mathbf{G}_{I_{mc}}$ ,  $\mathbf{G}_{P_{mc}}$  and  $\mathbf{G}_{D_{mc}}$  are the  $n_{mc} \times n_{mc}$  matrices given by

$$\begin{aligned} \mathbf{G}_{I_{mc}} &= \text{diag}(G_{I_1}, G_{I_2}, \dots, G_{I_{n_{mc}}}) \\ \mathbf{G}_{P_{mc}} &= \text{diag}(G_{P_1}, G_{P_2}, \dots, G_{P_{n_{mc}}}) \\ \mathbf{G}_{D_{mc}} &= \text{diag}(G_{D_1}, G_{D_2}, \dots, G_{D_{n_{mc}}}) \end{aligned} \quad (30)$$

Also,  $\mathbf{y}_{mc}(t)$ ,  $\dot{\mathbf{y}}_{mc}(t)$  and  $\ddot{\mathbf{y}}_{mc}(t)$  refer to  $n_{mc} \times 1$  modal displacement, modal velocity and modal acceleration vectors of the selected  $n_{mc}$  modes, respectively. The relationship between  $\mathbf{W}_{mc}(t)$  and  $\mathbf{W}_c(t)$  can be described by

$$\mathbf{W}_c(t) = \Psi \mathbf{W}_{mc}(t) \quad (31)$$

Where  $\Psi$  is a  $3n_c \times 3n_{mc}$  matrix which is given by

$$\Psi = \begin{bmatrix} \phi & \mathbf{0} & \mathbf{0} \\ \mathbf{0} & \phi & \mathbf{0} \\ \mathbf{0} & \mathbf{0} & \phi \end{bmatrix} \quad (32)$$

where  $n_c$  is the number of actuators ( the number of controlled stories) and  $\phi$  is the  $n_c \times n_{mc}$  matrix which is obtained through removing the rows corresponding to uncontrolled stories of the matrix  $\Phi_{mc}$ .

By substituting Eq. (7) in Eq. (27) and using Eq. (28), Eq. (33) is obtained.

$$\mathbf{G}_{mc} \mathbf{W}_{mc}(t) = \mathbf{E} \mathbf{G}_c \mathbf{W}_c(t) \quad (33)$$

where  $\mathbf{E} = \Phi_{mc}^T \mathbf{D}$  is the  $n_{mc} \times n_c$  modal participation matrix.

By substituting Eq. (31) in Eq. (33), feedback gain matrix of the controller is given by

$$\mathbf{G}_c = \mathbf{E}^{-1} \mathbf{G}_{mc} \Psi^{-1} \quad (34)$$

If  $n_{mc} = n_c$ , the inverse of matrices  $\mathbf{E}$  and  $\Psi$  exist; but, if  $n_{mc} \neq n_c$ , the physical gain matrix  $\mathbf{G}_c$  can be approximated by getting a pseudo-inverse of these matrices according to Eq. (35).

$$\mathbf{G}_c = \begin{cases} \mathbf{E}^{-1} \mathbf{G}_{mc} \Psi^{-1} & \text{if } n_{mc} = n_c \\ \mathbf{E}^+ \mathbf{G}_{mc} \Psi^+ & \text{if } n_{mc} \neq n_c \end{cases} \quad (35)$$

Where

$$\mathbf{E}^+ = \begin{cases} (\mathbf{E}^T \mathbf{E})^{-1} \mathbf{E}^T, \Psi^+ = \Psi^T (\Psi \Psi^T)^{-1} & \text{if } n_{mc} > n_c \\ \mathbf{E}^T (\mathbf{E} \mathbf{E}^T)^{-1}, \Psi^+ = (\Psi^T \Psi)^{-1} \Psi^T & \text{if } n_{mc} < n_c \end{cases} \quad (36)$$

Finally, by substituting Eq. (36) to Eq. (35), the feedback gain matrix is obtained as follows.

$$\mathbf{G}_c = \begin{cases} \mathbf{E}^{-1} \mathbf{G}_{mc} \Psi^{-1} & \text{if } n_{mc} = n_c \\ (\mathbf{E}^T \mathbf{E})^{-1} \mathbf{E}^T \mathbf{G}_{mc} \Psi^T (\Psi \Psi^T)^{-1} & \text{if } n_{mc} > n_c \\ \mathbf{E}^T (\mathbf{E} \mathbf{E}^T)^{-1} \mathbf{G}_{mc} (\Psi^T \Psi)^{-1} \Psi^T & \text{if } n_{mc} < n_c \end{cases} \quad (37)$$

Figure 2 shows the block diagram of the proposed controller.

## NUMERICAL STUDIES

In order to evaluate the performance and robustness of the proposed controller in reducing the structural response under earthquake loading, an 11-story realistic building shown in Figure3, studied by Pourzeynali et al. (2007), is considered.

Structural parameters of the main structure are given by Table 1. Also, the classical damping matrix,  $\mathbf{C}$ , is assumed to be proportional to the mass and stiffness matrices as

$$\mathbf{C} = \frac{2\xi_i \omega_i \omega_j}{\omega_i + \omega_j} \mathbf{M} + \frac{2\xi_j}{\omega_i + \omega_j} \mathbf{K} \quad (38)$$

where  $\omega_i$  and  $\omega_j$  are the structural frequencies in the  $i$ -th and  $j$ -th modes, respectively. Also,  $\xi_i$  and  $\xi_j$  are the structural damping ratios in the  $i$ -th and  $j$ -th modes, respectively.

TMD installed on the top story, modeled by linear springs and linear viscous dampers. The natural frequency of the TMD was tuned close to the first modal frequency of the main structure with a frequency ratio of  $\beta$ . The mass of the TMD system was chosen to be  $\alpha$ -percent of total mass of the building and damping ratio of the TMD was considered to be  $\xi$ - percent of the critical value. The optimal values of the TMD mass, damping and frequency ratios are generated by the genetic algorithm. These values obtained to be about 3%, 7% and 1.2, respectively. The optimum values of the ATMD are obtained by the genetic algorithm to be about 3%, 7% and 1.0, respectively.

In order to evaluate the simulation results, twelve performance indices, shown in Table 2, are divided into three categories: structural responses, control devices, and control strategy requirements. Performance indices  $J_1$  to  $J_6$ ,  $J_7$  to  $J_{10}$ , and  $J_{11}$  to  $J_{12}$  are related to structural responses, control devices, and control strategy requirements, respectively.

The maximum displacement of the top story in the controlled structure normalized to its corresponding value in the uncontrolled structure is shown by  $J_1$ . The uncontrolled structure is a structure with no control force feedback and control tools. On the other hand, the uncontrolled structure is the main structure equipped with the passive device, TMD, and the controlled structure is the main structure equipped with ATMD. Similarly, indices  $J_2$  to  $J_4$  represent the floors acceleration, stories drift, and base shear in the controlled structure normalized to their corresponding values in the uncontrolled structure, respectively. Indices  $J_5$  and  $J_6$  refer to values of the root mean squares (RMS) of the top story displacement and floors acceleration in the controlled structure normalized to their values in the

uncontrolled structure, respectively. The maximum and RMS of the actuator stroke in the controlled structure normalized to the maximum and RMS of the top story in the uncontrolled structure, are shown by indices  $J_7$  and  $J_8$ , respectively. Index  $J_9$  is the maximum control force generated by the actuator normalized by the total weight of the structure. Index  $J_{10}$  is presented to evaluate the required power to apply the control force. Index  $J_{11}$  is the total number of control sensors used for the control strategy. The number of required computational resources is given by index  $J_{12}$ . In fact, it is the dimension of discrete state vectors required for the control algorithm.

Two far-field (El Centro 1940 and Hachinohe 1968) and two near-field (Northridge 1994 and Kobe 1995) ground accelerations are selected to evaluate the proposed control strategy in different load disturbance. The absolute peak ground accelerations (PGA) of these earthquake records are 0.3417, 0.2250, 0.8267 and 0.8178 g, respectively.

In general, the nominal model is used for design conventional control system. Most often, the frequency of the first mode of the main structure has a dominant role in the dynamic response. Hence, a TMD/ATMD must be tuned for this frequency. Due to model errors, however, this frequency cannot be accurately determined. Also, this frequency changes during extreme dynamic events such as strong ground motions. Robust controllers are designed to function properly in the presence of bounded modeling errors or disturbances. In other words, it can also work well under a different set of assumptions although it designed for a particular set of parameters. To evaluate the robustness of the proposed controller in present to modeling uncertainty, the perturbation of story stiffness is treated for the example building. In this study,  $\delta_k = \pm 15\%$  perturbation of story stiffness is assumed.

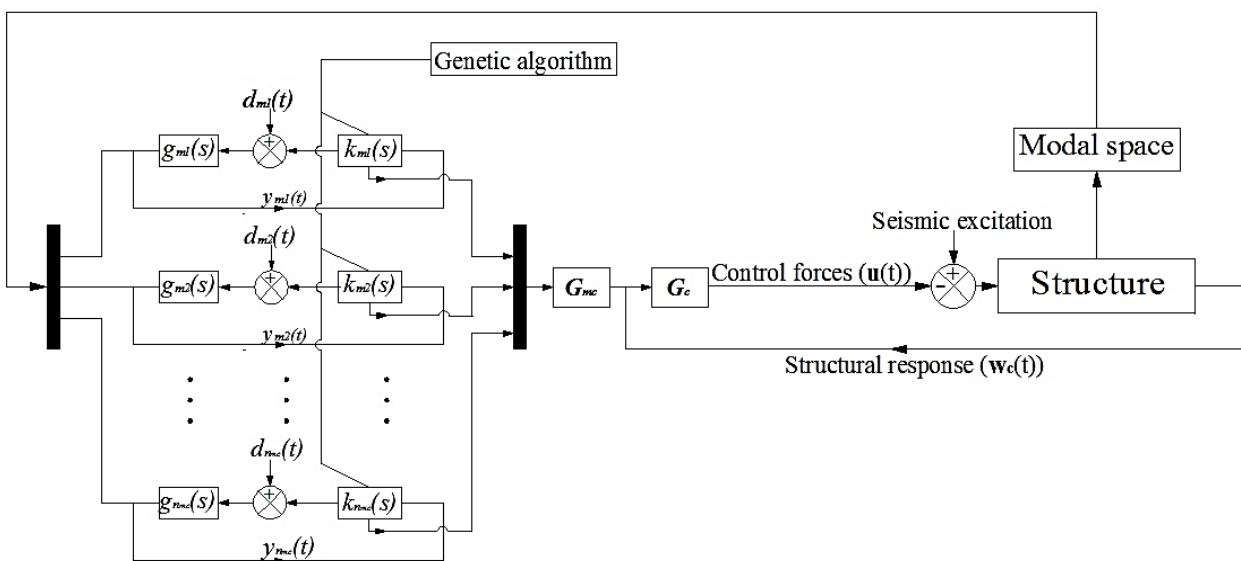
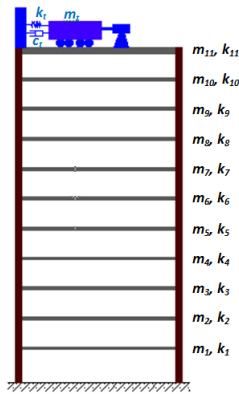


Figure 2. Schematic block diagram of the proposed controller



**Figure.3** The realistic building model equipped with the ATMD

**Table 1** Parameters of the main structure

Stories	Mass (kg)	Stiffness (N/m)
1	2.15e5	4.68e8
2	2.01e5	4.76e8
3	2.01e5	4.68e8
4	2.00e5	4.50e8
5	2.01e5	4.50e8
6	2.01e5	4.50e8
7	2.01e5	4.50e8
8	2.03e5	4.37e8
9	2.03e5	4.37e8
10	2.03e5	4.37e8
11	1.76e5	3.12e8

**Table 2** Performance indices

Peak top story displacement* $J_1 = \frac{\max_t \ x_r(t)\ }{\max_t \ \hat{x}_r(t)\ }$	Peak floors acceleration* $J_2 = \frac{\max_{t,f} \ a_f(t)\ }{\max_{t,f} \ \hat{a}_f(t)\ }$	Peak inter story drift* $J_3 = \frac{\max_{t,f} \ d_f(t)\ }{\max_{t,f} \ \hat{d}_f(t)\ }$
Peak base shear* $J_4 = \frac{\max_t \ V_0(t)\ }{\max_t \ \hat{V}_0(t)\ }$	RMS top story displacement* $J_5 = \frac{\max_i \ \sigma_{sr}(t)\ }{\max_i \ \hat{\sigma}_{sr}(t)\ }$	RMS floors acceleration* $J_6 = \frac{\max_f \ \sigma_a(t)\ }{\max_f \ \hat{\sigma}_a(t)\ }$
Maximum Control Device Stroke* $J_7 = \frac{\max_t \ x_t(t)\ }{\max_t \ \hat{x}_r(t)\ }$	RMS stroke of ATMD* $J_8 = \frac{\max_f \ \sigma_{st}(t)\ }{\max_f \ \hat{\sigma}_{sr}(t)\ }$	Control force* $J_9 = \frac{\max_t \ u_{ATMD}(t)\ }{W}$
Control power* $J_{10} = \frac{\max_t \ P_t(t)\ }{\max_t \ \dot{x}(t)\  W}$	$J_{11}$ = Number of required sensors	$J_{12}$ = Required computational resources

$x_r$  = top story displacement;  $t$  = earthquake time;  $\hat{\phantom{x}}$  = corresponding response quantity in the uncontrolled case;  $0 \leq t \leq T$ ;  $\|\phantom{x}\|$  = vector magnitude;  $f$  = floor number, 1, ..., 11;  $a_f$  = floor acceleration;  $d_f$  = inter story drift;  $V_0$  = base shear;  $\sigma_{sr}$  = RMS top story displacement;  $\sigma_a$  = RMS floor acceleration;  $x_t$  = actuator stroke;  $\sigma_{st}$  = RMS actuator stroke;  $u_{ATMD}$  = control force generated by actuator;  $w$  = building weight;  $P_t$  = required power and  $\dot{x}$  = the maximum uncontrolled velocity of the levels relative to the ground.

**Table 3.** Parameters of second- order models with corresponding controller ones for three modes of the studied structure

Mode i	Parameters of second-order model in the i-th mode		Controller parameters in the i-th mode		
	$\omega_i$	$\xi_i$	$G_{I_{mi}}$	$G_{P_{mi}}$	$G_{D_{mi}}$
i=1	5.804	0.050	405.079	7.6562	1.830
i=2	7.390	0.050	82.368	1.743	0.837
i=3	19.433	0.082	0.364	0.025	0.001

In this study, to determine the parameters of PID controller in each mode, the objective function is defined as

$$\begin{cases} \text{Min} & I_i = \sum_{k=1}^7 w_k I_k = w_1 I_1 + w_2 I_2 + w_3 I_3 + w_4 I_4 + w_5 I_5 + w_6 I_6 + w_7 I_7 \\ \text{S.t} & M_{si} - 1.6 \leq 0 \end{cases} \quad (39)$$

where  $w_k$  ( $k=1, \dots, 7$ ) are weighting factors.  $I_1$ ,  $I_2$  are the maximum top story modal displacement and acceleration of controlled second-order model in the i-th

mode normalized by them corresponding values in the uncontrolled second-order model.  $I_3$  is modal stories drift of controlled second-order model in the i-th mode normalized by its corresponding value in the uncontrolled one. Moreover, to evaluate the proposed controller based on required control resources, this, the non-dimensional performance indices  $I_4$ ,  $I_5$ ,  $I_6$  and  $I_7$  are defined.  $I_4$  is the maximum control force of second-order models normalized by the maximum base shear in the controlled second-order model. The RMS of the actuator

displacement, actuator velocity, and actuator absolute acceleration of the controlled second-order model in the  $i$ -th mode normalized by them corresponding values in the uncontrolled second-order models are shown by  $I_5$ ,  $I_6$  and  $I_7$ , respectively. The required physical size of the actuator is evaluated by  $I_5$ . Similarly, the required control power is assessed by  $I_6$ . Also, the magnitude of the control force is evaluated by  $I_7$ .

The optimization problem can be turned into an unconstrained one considering the following equation

$$I_i = w_1 I_{1i} + w_2 I_{2i} + w_3 I_{3i} + w_4 I_{4i} + w_5 I_{5i} + w_6 I_{6i} + w_7 I_{7i} + w_8 M_{si} \quad (40)$$

In this study,  $w_1=w_2=20$ ,  $w_3=10$ ,  $w_4=100$  and  $w_5=w_6=w_7=5$  are set. Thus, more attention is paid to the minimization of the maximum displacement and acceleration and demand control force. Also,  $w_7=0$  if the constraint in Eq. (39) is satisfied. Otherwise, it is set to be  $w_8=100$ . The generation histories of optimization process for the first three modes are shown in Fig.4.

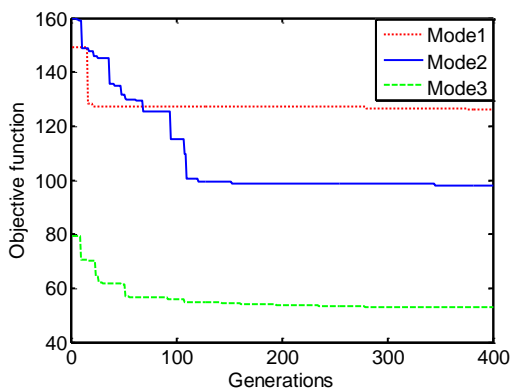


**Figure 4.** The generation histories of optimization process for the first three modes

It can be seen that the convergence of the objective function has been achieved in 150 generations; however, all of the genetic operations is repeated up to about 400 iterations for obtaining the converged optimal solution. The Parameters of second-order models corresponding with these modes are listed in Table 3. Also, considering the result of optimization procedure based on GA for the first three modes, parameters of controllers for these modes of the studied structure are presented in this table. It is remarkable that the values of

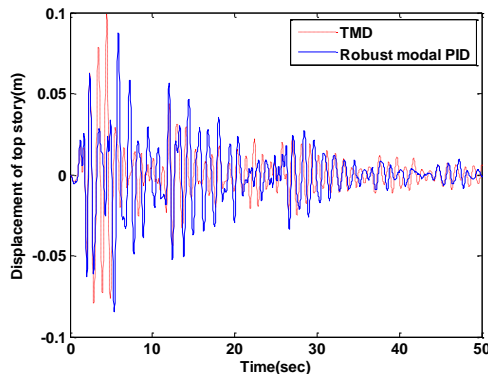
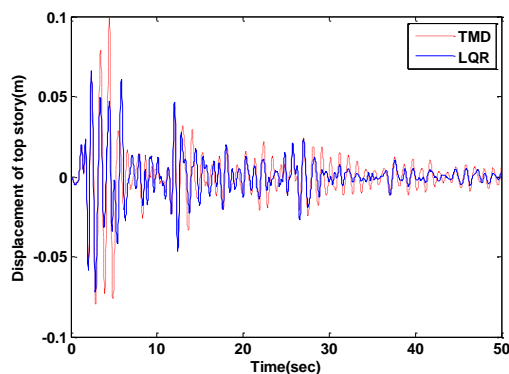


**Figure5.** Comparison of time histories of top story displacement of the nominal controlled structure using LQR and proposed controller with the uncontrolled structure subjected to El Centro earthquake

the control gains in the first mode are larger than the corresponding values in other modes. It means that the participation of higher modes to determine feedback gain matrix of controller control gains are less than that of fundamental mode of the structure. By tuning the parameters of PID controller in the controlled modes of the structure, the modal feedback gain matrix  $\mathbf{G}_{mc}$  is given by Eq. (29). By substituting  $\mathbf{G}_{mc}$  in Eq. (37), the feedback gain matrix of controller  $\mathbf{G}_c$  is obtained.

## RESULT AND DISCUSSION

The time history of the nominal structure is analyzed to evaluate the performance of proposed controller. The time history of the top story displacement and acceleration of the structure controlled by LQR and the proposed controller are compared with corresponding uncontrolled ones, as shown in Figs. 5 and 6 for El Centro earthquake. The uncontrolled structure is a structure with no control force feedback and control tools, namely the building equipped with TMD. Considering El Centro earthquakes, the time history of the required control force using LQR and robust modal PID controller are shown in Fig.7. Furthermore, compared with corresponding uncontrolled structure, the time history of the top story displacement and acceleration of the structure subjected to Kobe earthquake controlled by LQR and the proposed controller are illustrated in Figs 8 and 9. Also, the time history of the required control force using LQR and robust modal PID controller for this earthquake are shown in Fig.10. It can be seen from Figs. 5, 6, 8, and 9 that the proposed controller performs better in reducing displacement and acceleration of the top story than the LQR. Also it can be seen from Figs. 7 and 10 that the maximum required active control force for the proposed controller is about 635 KN while this value is 420 KN for LQR controller. These values are about 1419 and 1526 KN in Kobe earthquake.

In order to evaluate the performance and robustness of LQR and the proposed controller, the values of performance indices  $J_1$  to  $J_{10}$  are listed in Tables 4, 5, 6 and 7 for El Centro, Kobe, Hachinohe and Northridge earthquake, respectively. These values are for three structural models: nominal Model, perturbed model 1 ( $\delta_k=+0.15$ ) and perturbed model 2 ( $\delta_k=-0.15$ ).

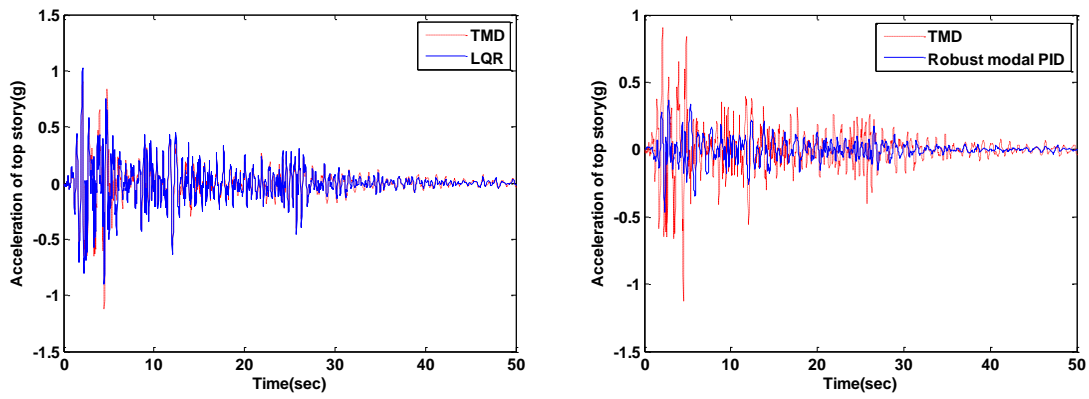


**Figure6.** Comparison of time histories of top story acceleration of the nominal controlled structure using LQR and proposed controller with the uncontrolled structure subjected to El Centro earthquake

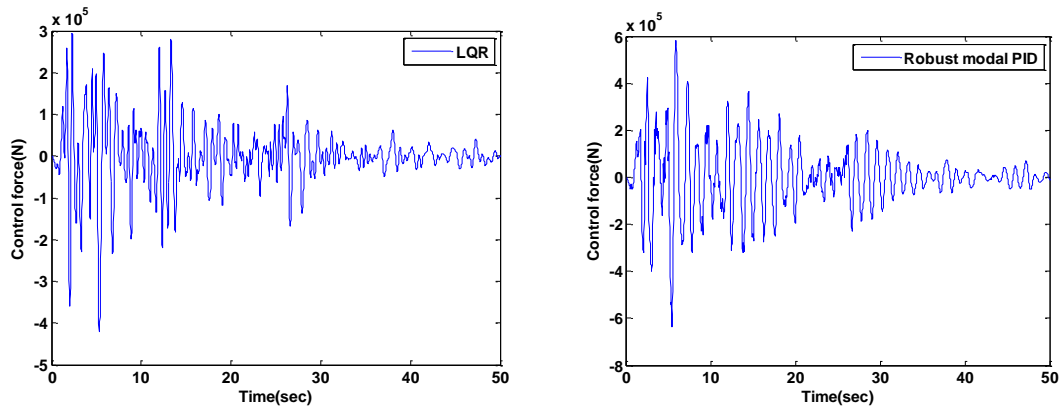


**Figure7.** Comparison of demanded control force of the nominal structure subjected to El Centro earthquake using LQR and proposed controller

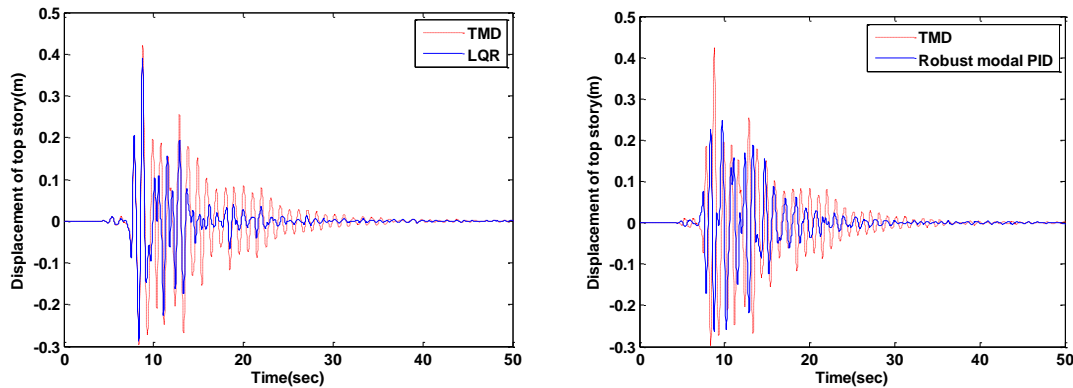


**Figure8.** Comparison of time histories of top story displacement of the nominal controlled structure using LQR and proposed controller with the uncontrolled structure subjected to Kobe earthquake

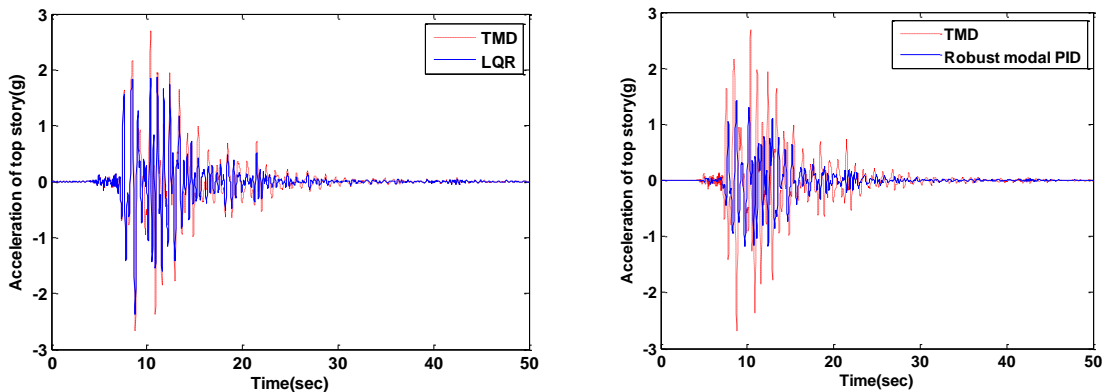


**Figure9.** Comparison of time histories of top story acceleration of the nominal controlled structure using LQR and proposed controller with the uncontrolled structure subjected to Kobe earthquake

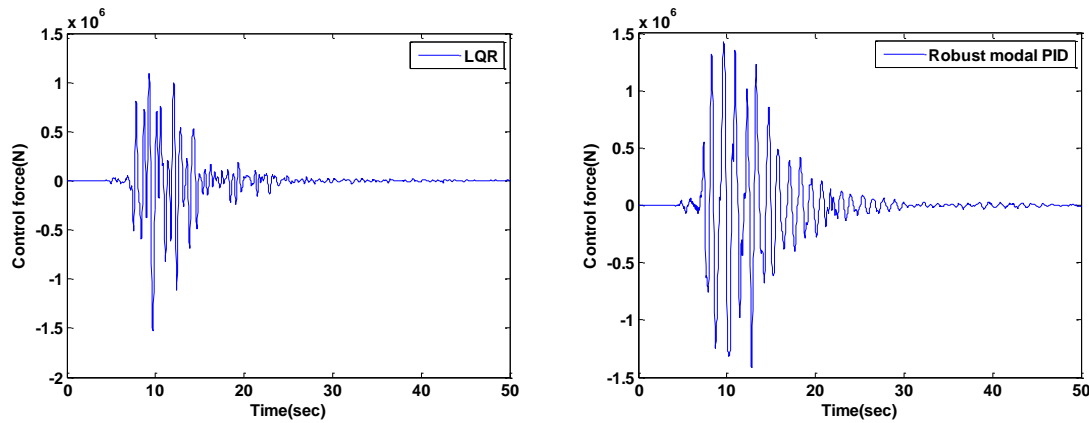


**Figure10.** Comparison of demanded control force of the nominal structure subjected to Kobe earthquake using LQR and proposed controller

**Table 4.** Performance indices of the Structural models subjected El Centro earthquake

Models	Controller	J <sub>1</sub>	J <sub>2</sub>	J <sub>3</sub>	J <sub>4</sub>	J <sub>5</sub>	J <sub>6</sub>	J <sub>7</sub>	J <sub>8</sub>	J <sub>9</sub>	J <sub>10</sub>
Nominal model	LQR	0.73	0.90	0.65	0.96	0.67	0.90	3.64	3.64	0.02	0.03
	Robust modal-PID	0.63	0.74	0.62	0.76	0.76	0.79	5.45	6.11	0.03	0.08
Perturbed model 1 ( $\delta_k=+0.15$ )	LQR	0.78	0.99	0.73	0.97	0.62	0.95	3.52	3.23	0.02	0.03
	Robust modal-PID	0.65	0.77	0.65	0.68	0.77	0.77	5.42	6.04	0.02	0.06
Perturbed model 2 ( $\delta_k=-0.15$ )	LQR	0.81	1.10	0.83	1.05	0.61	0.96	4.35	3.46	0.02	0.03
	Robust modal-PID	0.69	0.74	0.69	0.79	0.73	0.80	6.33	6.41	0.03	0.10

**Table 5.** Performance indices of the Structural models subjected Kobe earthquake

Models	Controller	J <sub>1</sub>	J <sub>2</sub>	J <sub>3</sub>	J <sub>4</sub>	J <sub>5</sub>	J <sub>6</sub>	J <sub>7</sub>	J <sub>8</sub>	J <sub>9</sub>	J <sub>10</sub>
Nominal model	LQR	0.93	0.86	0.87	0.83	0.80	0.84	4.08	3.21	0.07	0.17
	Robust modal-PID	0.63	0.71	0.68	0.87	0.74	0.82	5.29	5.13	0.07	0.29
Perturbed model 1 ( $\delta_k=+0.15$ )	LQR	0.87	0.84	0.84	0.96	0.61	0.74	3.81	3.18	0.07	0.15
	Robust modal-PID	0.67	0.70	0.67	0.78	0.65	0.75	5.57	4.85	0.06	0.30
Perturbed model 2 ( $\delta_k=-0.15$ )	LQR	1.03	0.94	0.99	1.10	0.78	0.89	4.39	4.39	0.07	0.17
	Robust modal-PID	0.69	0.73	0.72	0.86	0.86	0.89	6.27	7.11	0.10	0.37

**Table 6.** Performance indices of the Structural models subjected Hachinohe earthquake

Models	Controller	J <sub>1</sub>	J <sub>2</sub>	J <sub>3</sub>	J <sub>4</sub>	J <sub>5</sub>	J <sub>6</sub>	J <sub>7</sub>	J <sub>8</sub>	J <sub>9</sub>	J <sub>10</sub>
Nominal model	LQR	0.83	0.81	0.92	1.03	0.80	0.72	3.90	2.85	0.01	0.04
	Robust modal-PID	0.69	0.70	0.69	0.70	0.53	0.57	5.23	5.03	0.02	0.09
Perturbed model 1 ( $\delta_k=+0.15$ )	LQR	0.92	0.91	0.94	1.01	0.52	0.58	3.71	2.80	0.01	0.04
	Robust modal-PID	0.72	0.70	0.73	0.66	0.72	0.65	5.35	6.03	0.02	0.09
Perturbed model 2 ( $\delta_k=-0.15$ )	LQR	0.87	0.93	0.96	1.07	0.50	0.62	4.16	2.99	0.01	0.05
	Robust modal-PID	0.65	0.75	0.78	0.73	0.50	0.63	5.71	4.87	0.02	0.10

**Table 7.** Performance indices of the Structural models subjected Northridge earthquake

Models	Controller	J <sub>1</sub>	J <sub>2</sub>	J <sub>3</sub>	J <sub>4</sub>	J <sub>5</sub>	J <sub>6</sub>	J <sub>7</sub>	J <sub>8</sub>	J <sub>9</sub>	J <sub>10</sub>
Nominal model	LQR	0.95	0.92	0.82	0.99	0.74	0.92	4.93	3.83	0.05	0.10
	Robust modal-PID	0.74	0.79	0.70	0.74	0.76	0.79	6.41	6.31	0.08	0.19
Perturbed model 1 ( $\delta_k=+0.15$ )	LQR	1.03	1.13	0.98	1.11	0.87	0.82	4.99	3.80	0.05	0.09
	Robust modal-PID	0.76	0.76	0.73	0.73	0.81	0.83	6.71	6.81	0.07	0.20
Perturbed model 2 ( $\delta_k=-0.15$ )	LQR	0.96	1.07	0.93	1.02	0.86	0.88	4.71	3.82	0.05	0.11
	Robust modal-PID	0.73	0.64	0.75	0.76	0.79	0.88	6.82	6.91	0.09	0.22

It can be seen from simulation results that the proposed controller can reduce  $J_1$ , the performance index related to the maximum top story displacement, more than the LQR in all earthquakes. Considering perturbed model 2, for example,  $J_1$  for LQR and robust modal PID controller are 0.81 and 0.69 for El Centro earthquake. It means that in comparison with the LQR, the proposed

controller gives a reduction of 15%. Similarly, this reduction is 33%, 25% and 24%, for Kobe, Hachinohe and Northridge earthquakes, respectively. It is worth mentioning that LQR controller can reduce  $J_5$ , the performance index related to the RMS of the top story displacement, better than the proposed controller in some earthquakes.

Simulation results show that the proposed controller performs better than LQR controller in reduction of  $J_2$  which related to the peak floors acceleration. Also, in comparison with LQR controller, the proposed controller performs better in reduction of  $J_6$ , the performance index related to RMS of the absolute floors acceleration, in most earthquakes. Furthermore, considering  $J_4$ , the performance index related to the maximum base shear, it can be seen that the base shear of the structure is decreased using the proposed controllers.

Considering  $J_3$ , it can also be seen that the proposed controllers are able to reduce maximum drift stories of the structures better than the LQR. Considering perturbed model 1, for example, this reduction is 11%, 20%, 22% and 26%, for El Centro, Kobe, Hachinohe and Northridge earthquakes, respectively.

Considering index  $J_7$  and  $J_8$ , it can be observed that the proposed controller needs more physical space for the movement of ATMD. Also, considering index  $J_9$  and  $J_{10}$ , it can be seen that the robust modal PID controllers demand higher control forces and external powers. In fact, the LQR in earthquakes with high PGA values, such as Kobe and Northridge cannot reduce structural responses well. However, the proposed controller is able to significantly reduce structural responses at the cost of increasing the required control force, stroke of the actuator and external power.

Considering  $J_1$ ,  $J_2$  and  $J_3$  which are related to major structural responses in Tables 5, 6, 7 and 8 for perturbed models, it can be seen the proposed controller in present to modeling uncertainty has maintained its good performance. However, the performance of the LQR in reducing these responses has often been deteriorated.

The last two criteria for assessing controllers are  $J_{11}$  and  $J_{12}$ , the total number of control sensors used to control structure as well as the required computational resources. To determine the demanded control force by the LQR controller, it is needed to estimate the displacement, velocity and acceleration states. Therefore, one sensor and two computational resources are required for each degree of freedom of the structure. Hence, for the benchmark structure the values of  $J_{11}$  and  $J_{12}$  are 12 and 24, respectively. To adjust the control force required for the proposed controller, it is needed to estimate displacement and velocity and acceleration of the top story. Therefore, the values of  $J_{11}$  and  $J_{12}$  are 1 and 2. As a result, because of the limitation in the number of required sensors for adjusting control force, the proposed controller is a simple control system for large structures in comparison with conventional modern control methods such as LQG and LQR. This means the proposed control strategy offers advantages in terms of reliability and cost.

## CONCLUSIONS

In this paper, a robust modal-PID controller was developed for seismic control of structures.  $n$  coupled equations of motion of an  $n$ -degree-of-freedom structure were transformed into a set of  $n$  decoupled equations in the modal coordinates. For creating a balance between performance and robustness of the controller, the modal

feedback gain of controller in the reduced modal space was designed using genetic algorithm. Then, based on the contribution of the modal responses to the structural response, the gain feedback matrix of controller of structure was obtained. The proposed controller was used for adjusting active control force of an ATMD installed on top story of an 11-story realistic building subjected to seismic excitations. Four earthquakes and twelve performance indices were taken into account to investigate the performance of the proposed controllers. To assess robustness of the proposed controller in present to modeling uncertainty, the perturbation of story stiffness is treated for the example building.

The simulation results showed that the proposed controller performed better than LQR in terms of terms of reduction of the maximum top story displacement, maximum stories acceleration as well as maximum stories drift. Furthermore, the simulation results demonstrated the LQR controller does not have a good performance in earthquakes with high PGA values, but the proposed controller is able to significantly reduce structural responses at the cost of demanding a higher control force and external power. Additionally, the proposed controller was not sensitive to modeling errors. On the other words, it was capable maintain a desired performance in dealing with uncertainties. One of the advantages of the proposed controller was that the controller required only one sensor and two computational resources to regulate control force of actuator in real time. Therefore, in comparison with conventional modern control, the proposed controller provided a simple strategy to adjust control force in tall building. It means that the proposed controller had superior in terms of reliability and cost.

## REFERENCES

1. Aguirre, N.; Ikhouane, F.; Rodellar J. (2011). Proportional-plus-integral semi active control using magneto-rheological dampers. *Journal of Sound and Vibration*, 330(10):2185–2200.
2. Astrom, K.J.; Hagglund, T. (1995). *PID Controllers: Theory, Design and Tuning*, ISA and Research Triangle, Par, NC.
3. Datta, T.K. (1996). Control of dynamic response of structures, *Indo-US symposium on emerging trends in vibration and noise engineering*, pp.18– 20.
4. Deb, K. (2001). *Multi-objective optimization using evolutionary algorithms*, John Wiley & Sons, UK.
5. Etedali, S.; Sohrabi, M.R.; Tavakoli S. (2013). Optimal PD/PID control of smart base isolated buildings equipped with piezoelectric friction dampers. *Earthquake Engineering and Engineering Vibration*, 12(1):39-54.
6. Fisco, N.R.; Adeli, H. (2011a). Smart structures: Part I-Active and semi-active control. *Scientia Iranica, Transaction A: Civil Engineering*, 18(3):275–284.
7. Fisco, N.R.; Adeli, H. (2011b). Smart structures: Part II—hybrid control systems and control strategies. *Scientia Iranica, Transaction A: Civil Engineering*, 18(3):285–295.
8. Fung, R.F.; Liu, Y.T.; Wang C.C. (2005). Dynamic model of an electromagnetic actuator for vibration

- control of a cantilever beam with a tip mass. *Journal of Sound and Vibration*, 288: 957-980.
9. Gu, D.W.; Petkov, P.Hr.; Konstantinov, M.M.(2005). *Robust Control Design with MATLAB. Advanced Textbooks in Control and Signal Processing*, Springer-Verlag Inc., London, England.
  10. Guclu, R. (2003). Fuzzy-logic control of vibrations of analytical multi-degree-of-freedom structural systems. *Turkish Journal of Engineering and Environmental Sciences*, 27(3): 157–167.
  11. Guclu, R. (2006). Sliding mode and PID control of a structural system against Earthquake. *Mathematical and Computer Modeling*, 44: 210–217.
  12. Guclu, R.; Yazici, H. (2007). Fuzzy-logic control of a non-linear structural system against earthquake induced vibration. *Journal Vibration Control*, 13(11): 1535–155.
  13. Guclu, R.; Yazici, H. 2009. Seismic-vibration mitigation of a nonlinear structural System with an ATMD through a fuzzy PID controller, *Nonlinear Dynamic* 58: 553–564.
  14. Ha, Q.P. (2001). Active structural control using dynamic output feedback sliding mode. *In: Proc. Australian conference on robotics and automation Sydney*, pp.14– 15.
  15. Huo, L.; Song, G.; Li, H.; Grigoriadis, K. (2008).  $H_\infty$  robust control design of active structural vibration suppression using an active mass damper. *Smart Material and Structures*, 17(1).
  16. Jung, W.J.; Jeong, W.B.; Hong, S.R.; Choi, S.B. (2004). Vibration control of a flexible beam structure using squeeze-mode ER mount. *Journal of Sound and Vibration*, 273(1-2):185-199.
  17. Kanai, K. (1961). An empirical formula for the spectrum of strong earthquake motions. *Bulletin Earthquake Research Institute*, 39:85-95.
  18. Nagarajaiah, S.; Narasimhan, S. (2006). Smart base-isolated benchmark building part II: phase I, sample controllers for linear and friction isolation. *Journal of Structural Control and Health Monitoring*, 13:589-604.
  19. Park, K.S.; Park, W.U. (2012). Min-max optimum design of active control system for earthquake excited structures. *Advances in Engineering Software*, 51:40-48.
  20. Panda, R.C.; Yu, C.C.; Huang, H.P. (2004). PID tuning rules for SOPDT systems: review and some new results. *ISA Transactions*, 43: 283–295.
  21. Pourzeynali, S.; Lavasani, H.H.; Modarayi, A.H. (2007). Active control of high rise building structures using fuzzy logic and genetic algorithms. *Engineering Structures*, 29(3):346-357.
  22. Sarbjeet, S.; Datta, T.K. (2000). Nonlinear sliding mode control of seismic response of building frames. *Journal of Engineering Mechanics, ASCE*, 126(4):340-347.
  23. Samali, B.; Al-Dawod, M. (2003). Performance of a five-story benchmark model using an active tuned mass damper and a fuzzy controller. *Engineering Structures*, 25(13):1597-610.
  24. Samali, B.; Al-Dawod, M.; Kwok, K.C.S.; Naghdy, F. (2004). Active control of cross wind response of 76-story tall building using a fuzzy controller. *Journal of Engineering Mechanics*, 130(4):492-498.
  25. Shen, Y.; Homaifar, A.; Chen, D. (2000). Vibration control of flexible structures using fuzzy logic and genetic algorithms, American, Chicago, IL, USA, vol.1, PP.448-452.
  26. Skogestad, S. (2004). Simple analytic rules for model reduction and PID controller tuning. *Modeling, identification and control*, 25:85-120.
  27. Tavakoli, S.; Griffin, I.; Fleming, P.J. (2006). Tuning of decentralized PI (PID) controllers for TITO processes. *Control Engineering Practice*, 14: 1069–1080.
  28. Tavakoli, S. (2005). Multivariable PID Control with Application to Gas Turbine Engines, PhD Thesis. University of Sheffield, UK.
  29. Tavakoli, S.; Griffin, I.; Fleming, P.J. (2005). Robust PI Controller for Load Disturbance Rejection and Set point Regulation, *Proceedings of the 2005 IEEE Conference on Control Applications*, Toronto, Canada, August 2005, PP.28-31.
  30. Yang, J.N.; Soong, T.T. (1988). Recent advances in active control of civil engineering structures. *Probabilistic Engineering Mechanics*, 3(4):179–188.